Supporting Information

Diiron Carbonyl Complexes Bearing an N,C,S-Pincer Ligand: Reactivity toward Phosphines, Heterolytic Fe–Fe Cleavage, and Electrocatalytic Proton Reduction

Masakazu Hirotsu,*[,†] Kiyokazu Santo,[†] Chiaki Tsuboi,[†] and Isamu Kinoshita[†,‡]

[†]Graduate School of Science and [‡]The OCU Advanced Research Institute for Natural Science and Technology (OCARINA), Osaka City University, Sumiyoshi-ku, Osaka 558-8585, Japan

E-mail: mhiro@sci.osaka-cu.ac.jp

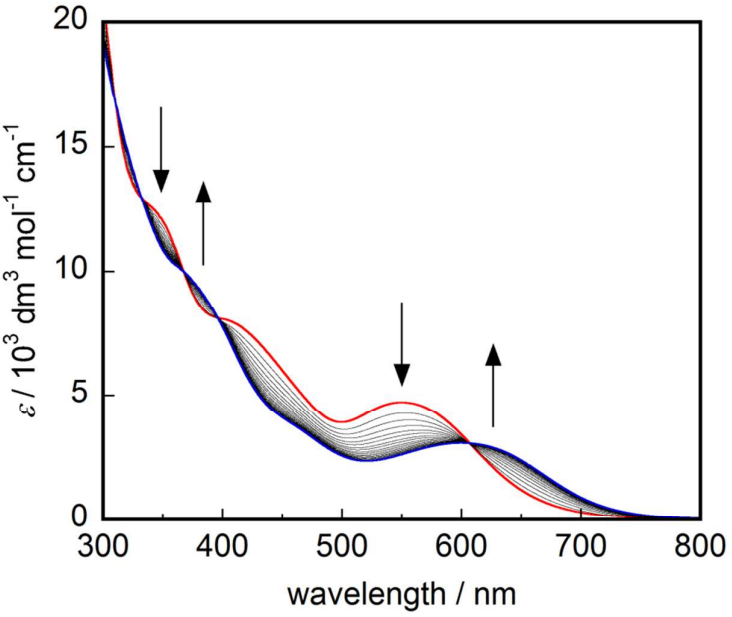

Figure S1. Electronic absorption spectral changes of **2** in THF (7.5×10^{-5} M, 27 °C). The spectrum was measured every 10 min for 3 h. The initial spectrum is shown in red. The isosbestic points are as follows: λ/nm (ε/dm^3 mol^{-1} cm^{-1}), 310 (17000), 334 (13000), 366 (10000), 399 (8100), 605 (3200).

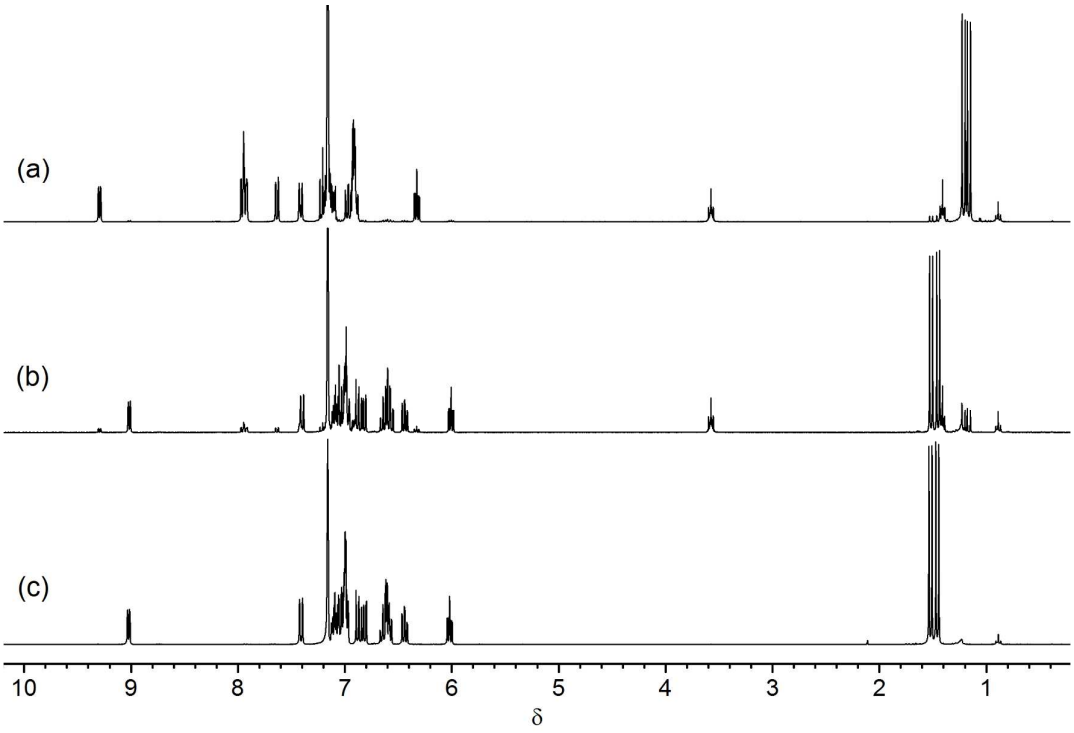

Figure S2. (a) ^{1}H NMR spectrum (300 MHz) of **2** in C_6D_6. (b) The C_6D_6 solution of **2** was heated at 60 °C for 1 h. (c) ^{1}H NMR spectrum (300 MHz) of **3** in C_6D_6.

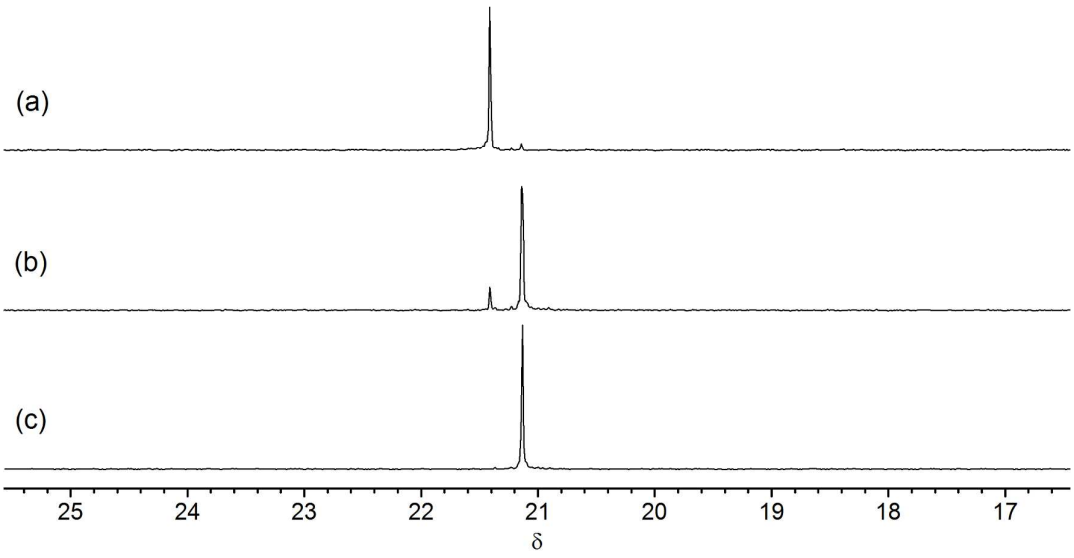

Figure S3. (a) $^{31}P\{^{1}H\}$ NMR spectrum (121.5 MHz) of **2** in C_6D_6. (b) The C_6D_6 solution of **2** was heated at 60 °C for 1 h. (c) $^{31}P\{^{1}H\}$ NMR spectrum (121.5 MHz) of **3** in C_6D_6.

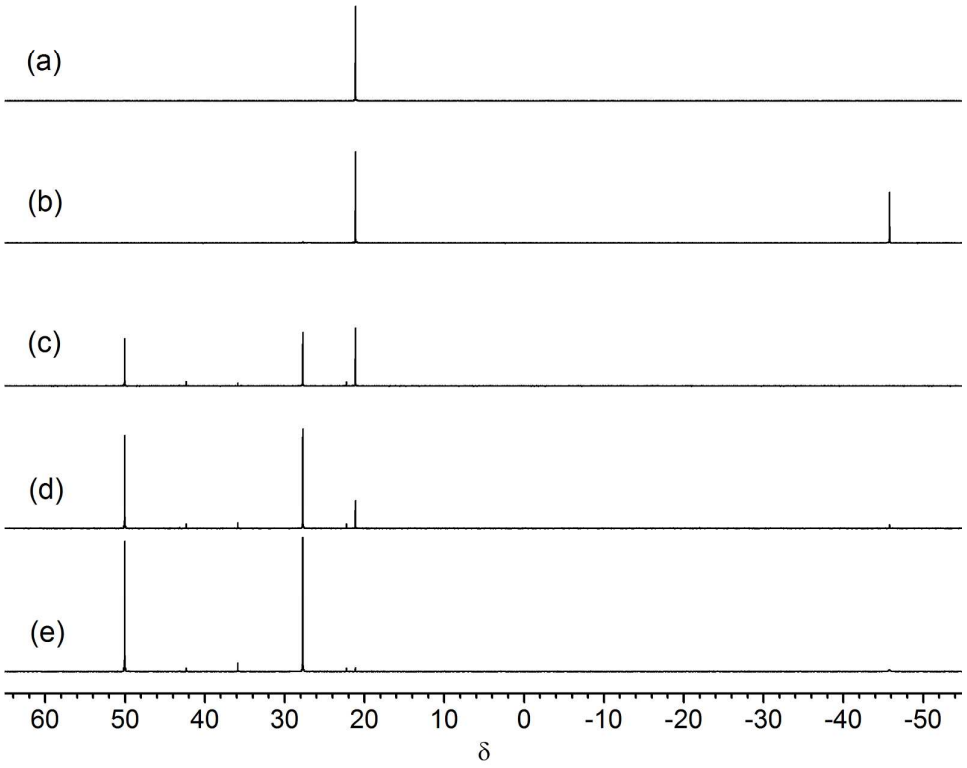

Figure S4. $^{31}P\{^{1}H\}$ NMR spectra (121.5 MHz, C_6D_6) of a reaction solution of **3** and PMe_2Ph in C_6D_6: (a) A solution of complex **3**. (b) One equiv of PMe_2Ph was added. (c) The solution was heated at 60 °C for 2 h. (d) One equiv of PMe_2Ph was added, and the solution was heated at 60 °C for 2 h. (e) One equiv of PMe_2Ph was added, and the solution was heated at 60 °C for 4 h.

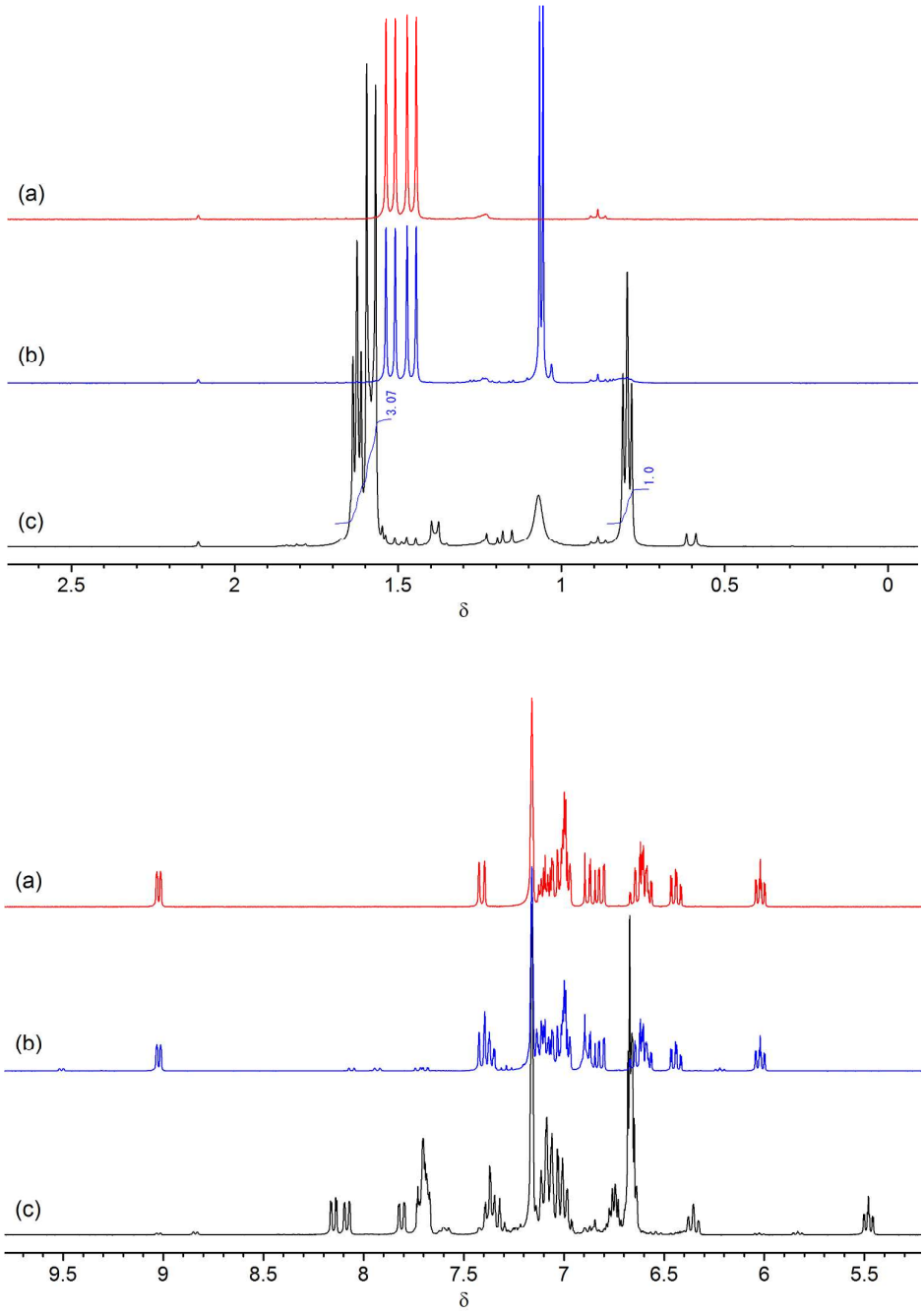

Figure S5. ^{1}H NMR spectra (300 MHz, C_6D_6) of a reaction solution of **3** and PMe_2Ph in C_6D_6: (a) A solution of complex **3**. (b) One equiv of PMe_2Ph was added. (c) The reaction solution of **3** and PMe_2Ph (3 equiv) was heated at 60 °C.

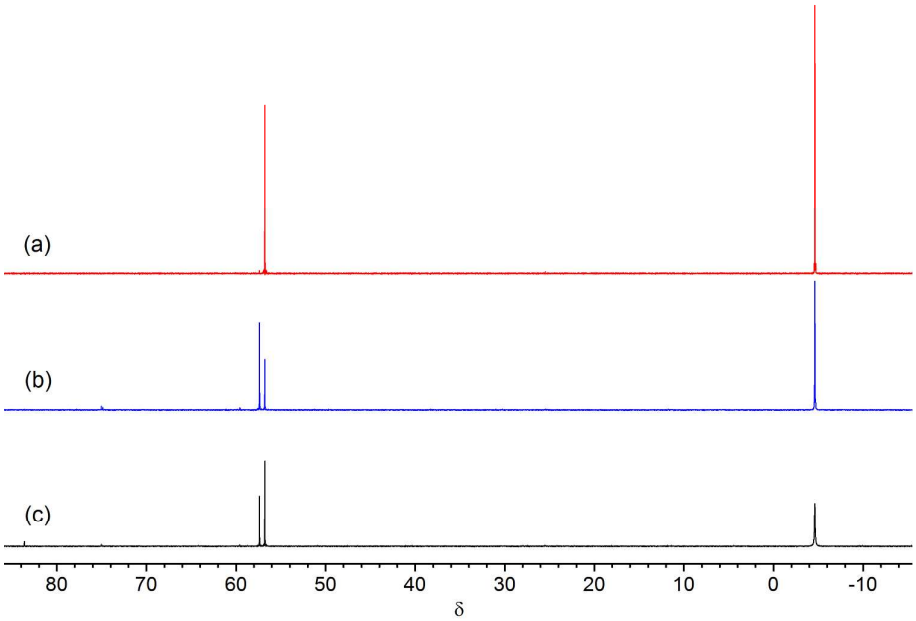

Figure S6. $^{31}P\{^{1}H\}$ NMR spectra (121.5 MHz, C_6D_6) of a reaction solution of **1** and PPh_3 in C_6D_6: (a) A 1:3 mixture of **1** and PPh_3. (b) The 1:3 mixture was heated at 60 °C for 6 h. (c) After 3 weeks at room temperature.

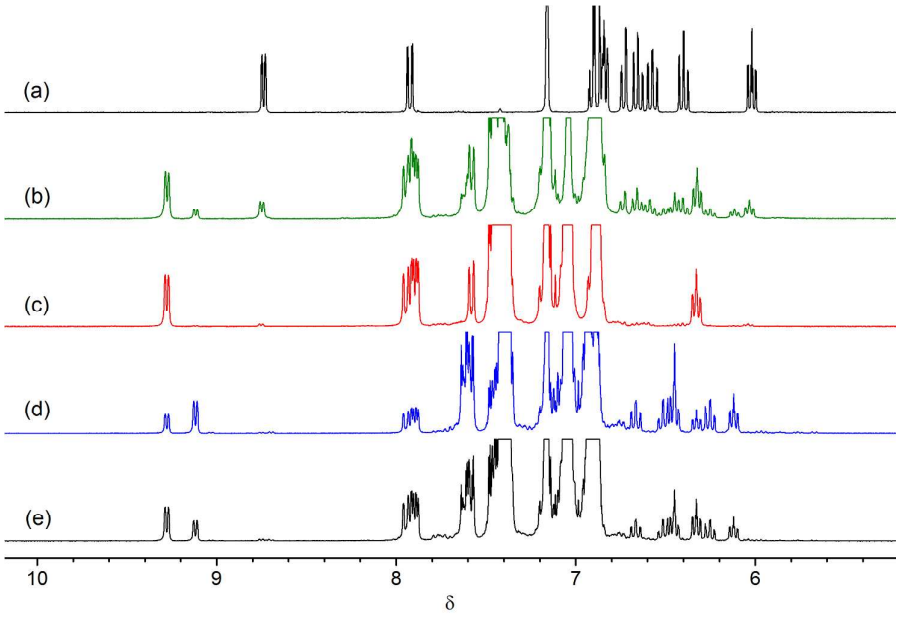

Figure S7. ^{1}H NMR spectra (300 MHz, C_6D_6) of a reaction solution of **1** and PPh_3 in C_6D_6: (a) A solution of complex **1**. (b) A 1:1 mixture of **1** and PPh_3 was stood at room temperature for 24 h. (c) A 1:3 mixture of **1** and PPh_3. (d) The 1:3 mixture was heated at 60 °C for 6 h. (e) After 3 weeks at room temperature.

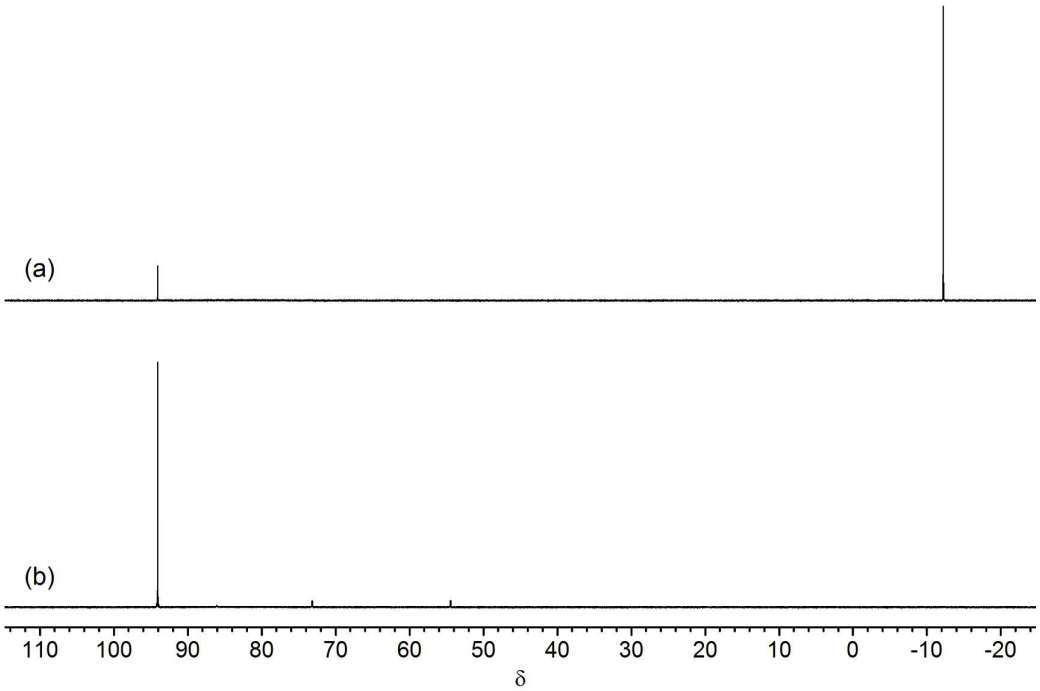

Figure S8. $^{31}P\{^{1}H\}$ NMR spectra (121.5 MHz, C_6D_6) of a reaction solution of **1** and dppbz (1:1) in C_6D_6: (a) After 24 h at room temperature. (b) After heating at 60 °C for 12 h.

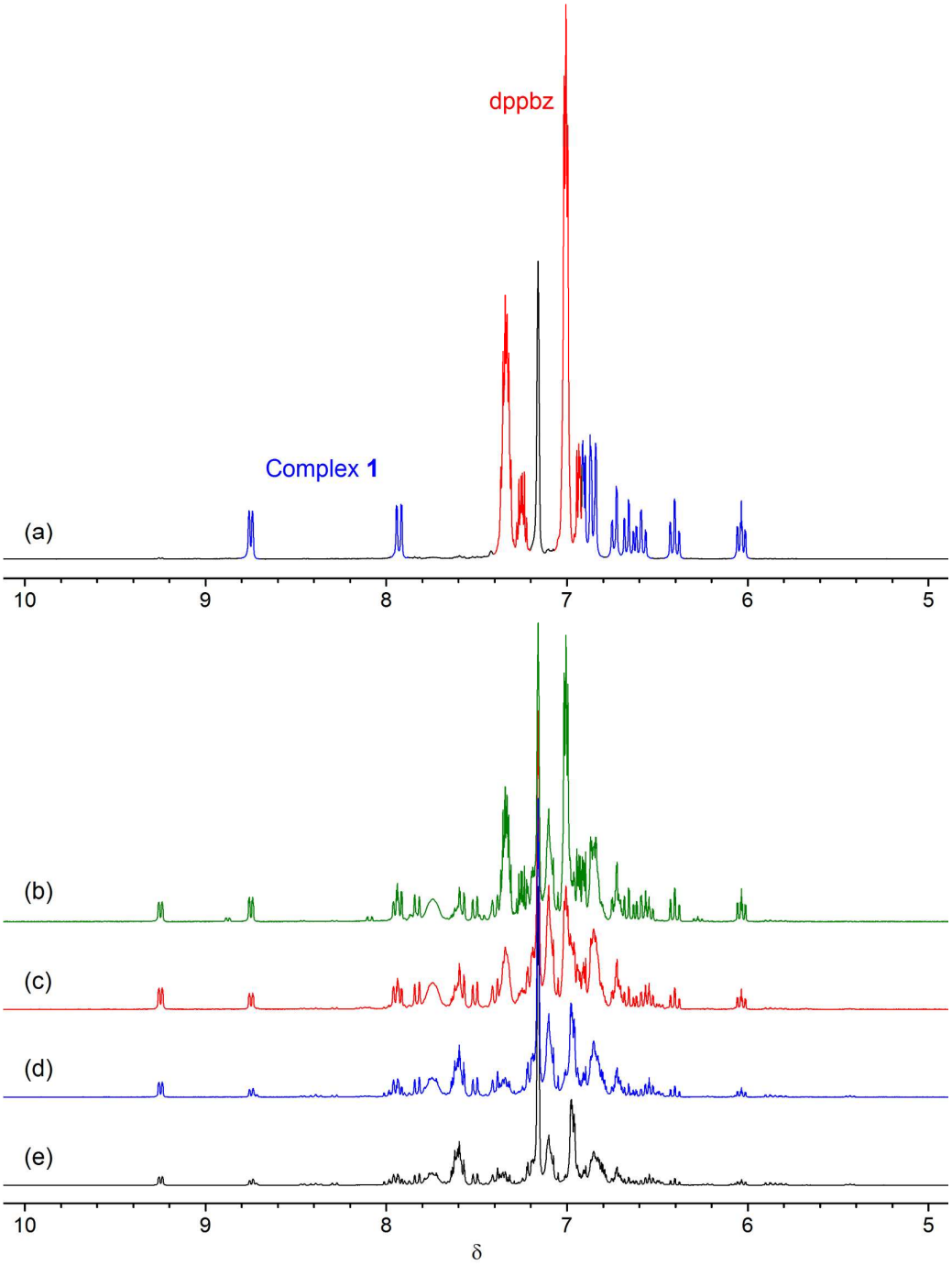

Figure S9. ^{1}H NMR spectra (300 MHz, C_6D_6) of a reaction solution of **1** and dppbz in C_6D_6: (a) A 1:1 mixture of **1** and dppbz. (b) After 24 h at room temperature. (c) After heating at 60 °C for 2 h. (d) After heating at 60 °C for 6 h. (e) After heating at 60 °C for 12 h.

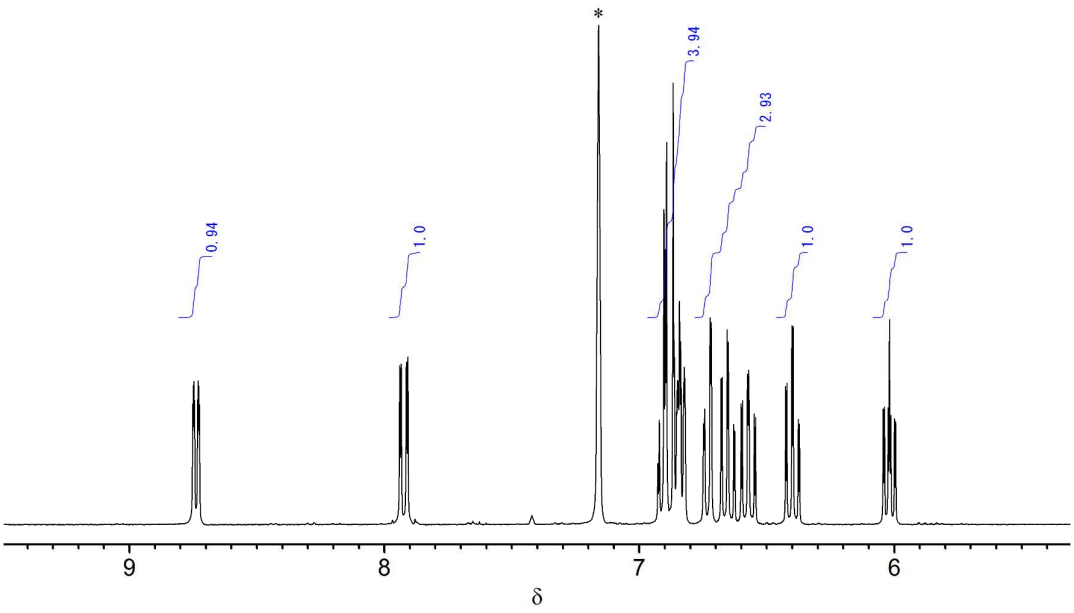

Figure S10. ^{1}H NMR spectrum (300 MHz, C_6D_6) of **1**. Residual solvent signals are marked with an asterisk.

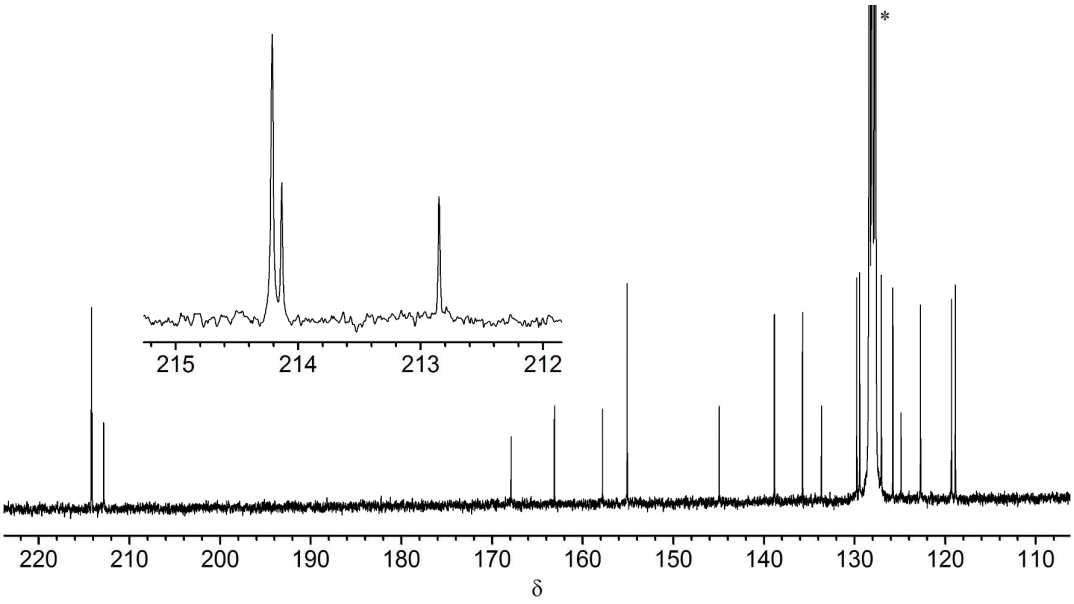

Figure S11. $^{13}C\{^{1}H\}$ NMR spectrum (75.5 MHz, C_6D_6) of **1**. Residual solvent signals are marked with an asterisk.

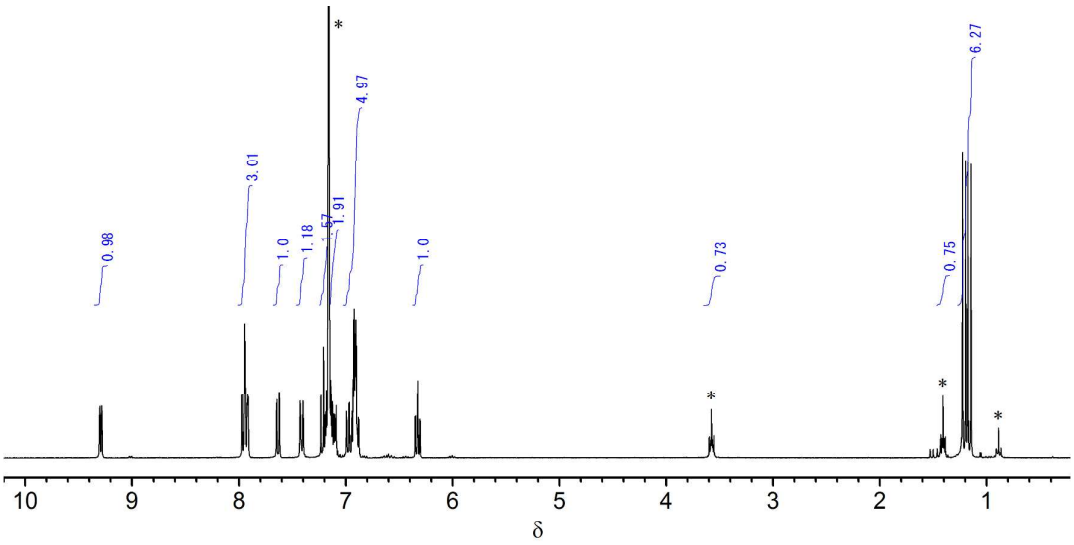

Figure S12. ^{1}H NMR spectrum (300 MHz, C_6D_6) of **2**. Residual solvent signals are marked with an asterisk.

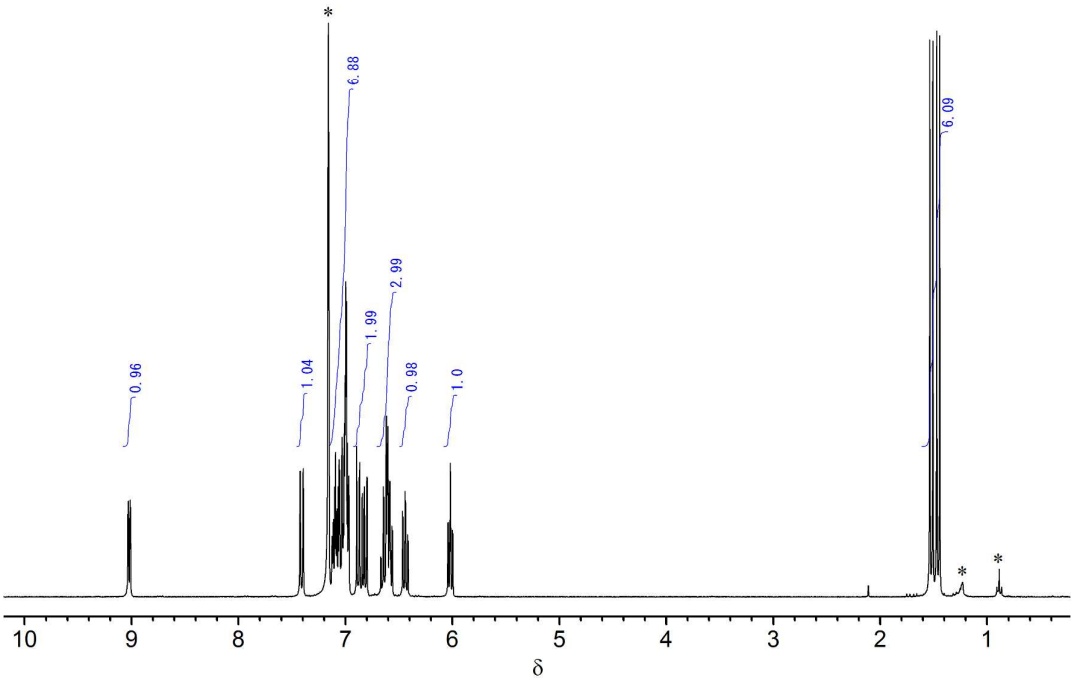

Figure S13. ^{1}H NMR spectrum (300 MHz, C_6D_6) of **3**. Residual solvent signals are marked with an asterisk.

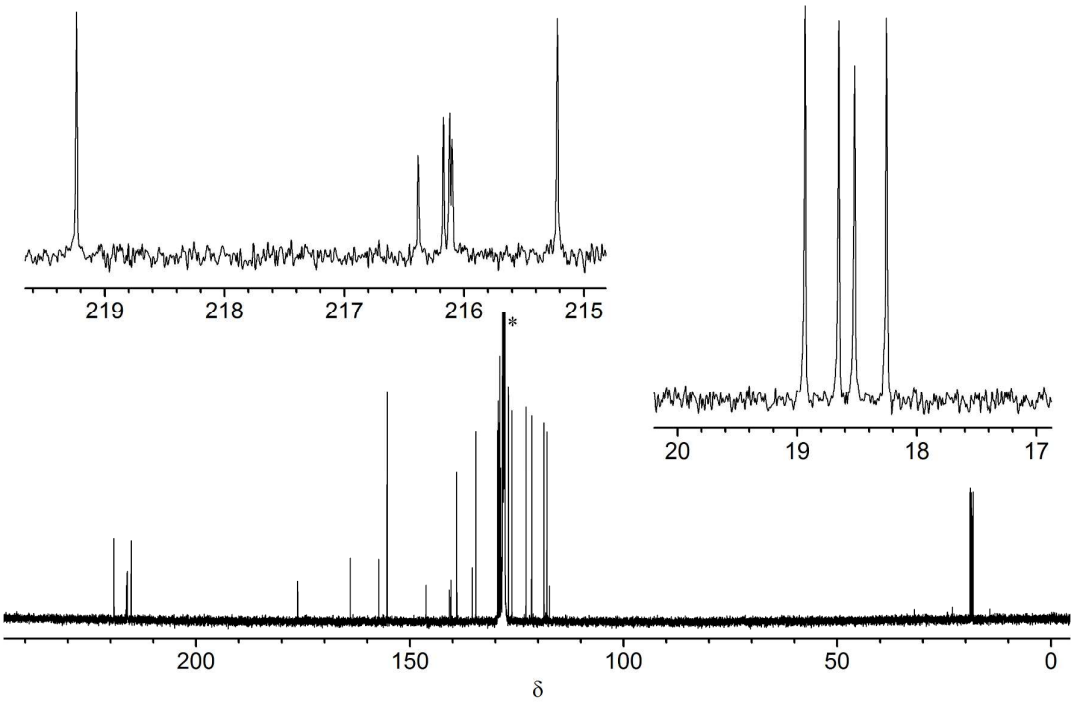

Figure S14. $^{13}C\{^{1}H\}$ NMR spectrum (100 MHz, C_6D_6) of **3**. Residual solvent signals are marked with an asterisk.

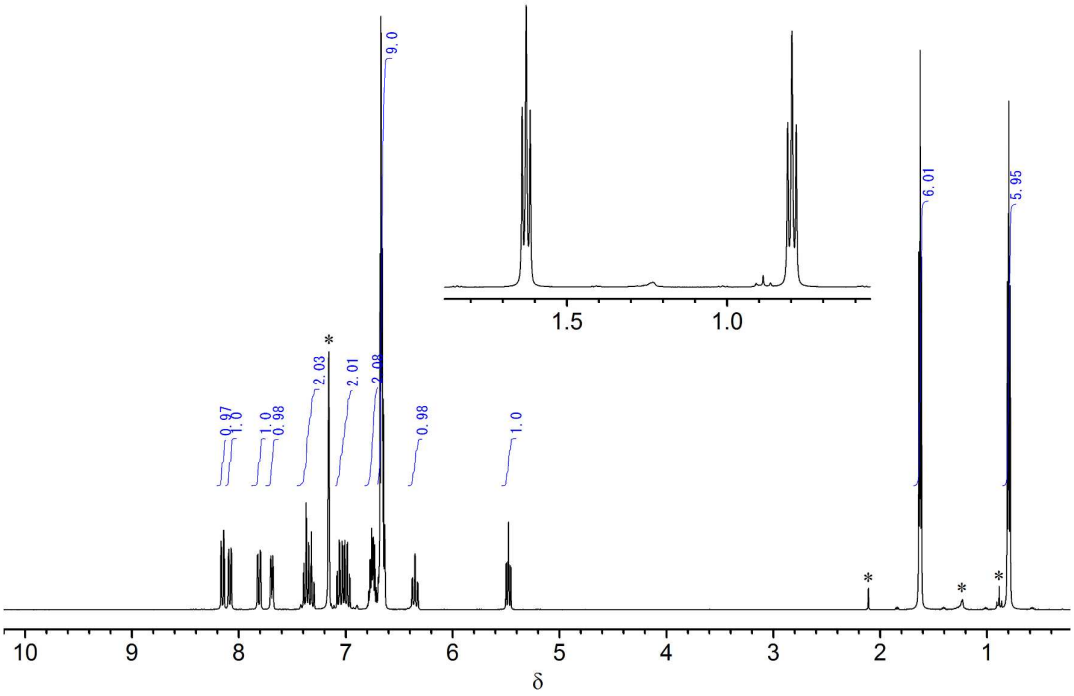

Figure S15. ^{1}H NMR spectrum (300 MHz, C_6D_6) of **4**. Residual solvent signals are marked with an asterisk.

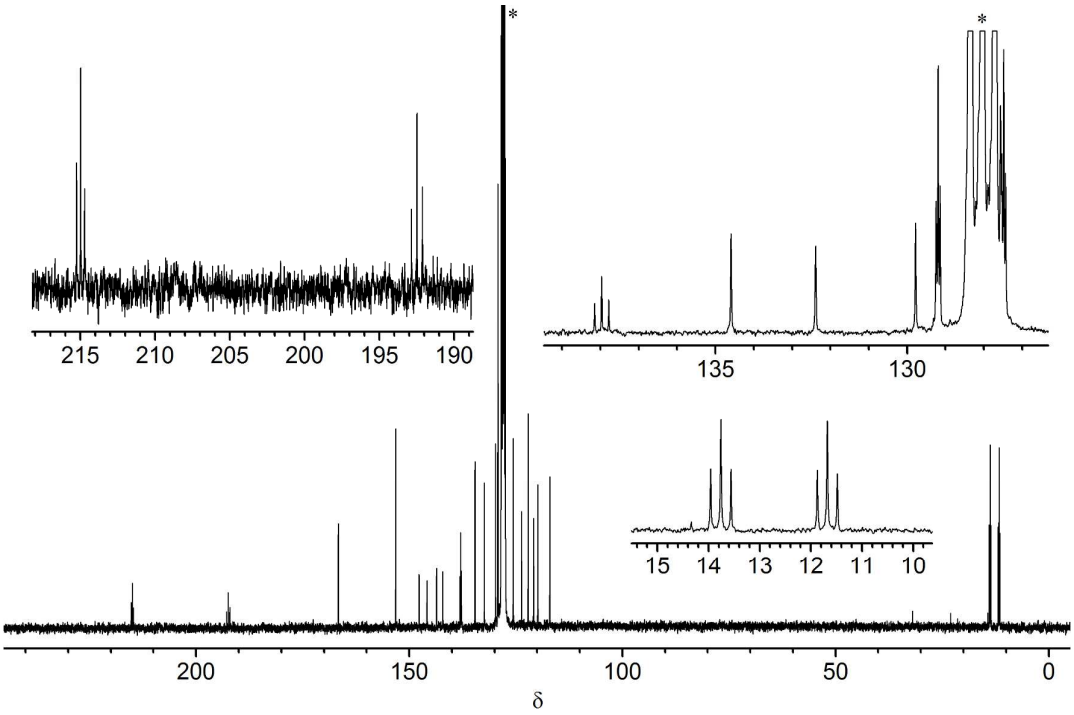

Figure S16. $^{13}C\{^{1}H\}$ NMR spectrum (75.5 MHz, C_6D_6) of **4**. Residual solvent signals are marked with an asterisk.

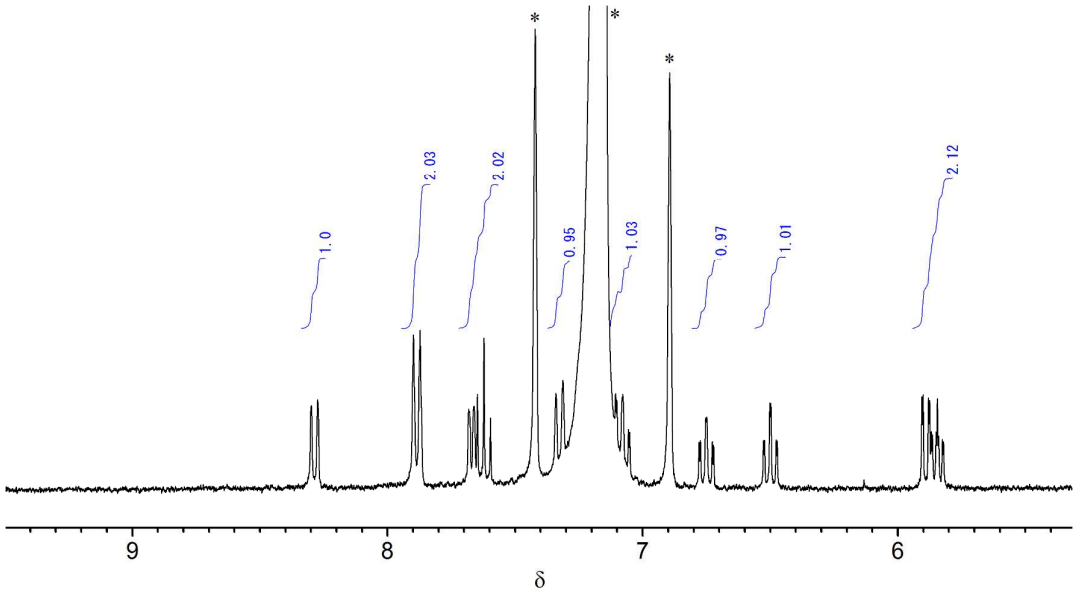

Figure S17. ^{1}H NMR spectrum (300 MHz, C_6D_6) of **7**. Residual solvent signals are marked with an asterisk.

Table S1. Crystallographic Data for **2** and **3**

	2	**3**
Empirical formula	$C_{30}H_{22}Fe_2NO_5PS$	$C_{29}H_{22}Fe_2NO_4PS$
Formula weight	651.23	623.22
Temperature/K	153	153
Wavelength/Å	0.7107	0.7107
Crystal system	monoclinic	monoclinic
Space group	$P2_1/n$	$P2_1/c$
a/Å	14.882(2)	13.6517(12)
b/Å	10.3475(15)	13.3882(11)
c/Å	18.878(3)	14.5907(12)
α/°	90	90
β/°	109.747(2)	94.790(2)
γ/°	90	90
V/Å^3	2736.1(7)	2657.5(4)
Z	4	4
D_{calcd}/Mg·m^{-3}	1.581	1.558
μ(Mo Kα)/mm^{-1}	1.237	1.267
F(000)	1328	1272
Crystal size/mm^3	0.16 × 0.15 × 0.12	0.34 × 0.14 × 0.07
Reflections collected	21963	25197
Independent reflections	6166 (R_{int} = 0.027)	5965 (R_{int} = 0.050)
Completeness to θ	98.2% (θ = 27.48°)	98.0% (θ = 27.48°)
Max. and min. transmission	0.8657 and 0.8266	0.9165 and 0.6726
No. of data/restraints/parameters	6166/0/449	5965/0/431
Goodness of fit on F^2	1.038	1.080
Final R indices [$I > 2\sigma(I)$]	R1 = 0.0357	R1 = 0.0440
R indices (all data)	wR2 = 0.0882	wR2 = 0.0928
Largest diff. peak and hole (e·Å^{-3})	0.704 and –0.316	0.367 and –0.362

Table S2. Crystallographic Data for **4** and **7**

	4	**7**
Empirical formula	$C_{34}H_{33}FeNOP_2S$	$C_{40}H_{26}Cl_4Fe_2N_2O_4S_2$
Formula weight	621.47	916.27
Temperature/K	193	193
Wavelength/Å	0.7107	0.7107
Crystal system	triclinic	monoclinic
Space group	$P\bar{1}$	$P2_1/a$
a/Å	10.1007(4)	16.1004(12)
b/Å	10.7986(7)	13.1729(9)
c/Å	15.3504(10)	18.3841(14)
α/°	86.390(7)	90
β/°	71.960(6)	106.263(2)
γ/°	70.393(5)	90
V/Å^3	1498.13(15)	3743.0(5)
Z	2	4
D_{calcd}/Mg·m^{-3}	1.378	1.626
μ(Mo Kα)/mm^{-1}	0.708	1.218
F(000)	648	488
Crystal size/mm^3	0.24 × 0.21 × 0.11	0.21 × 0.21 × 0.19
Reflections collected	14355	34864
Independent reflections	6400 (R_{int} = 0.023)	8433 (R_{int} = 0.038)
Completeness to θ	93.1% (θ = 27.49°)	98.4% (θ = 27.49°)
Max. and min. transmission	0.9262 and 0.8484	0.8015 and 0.7839
No. of data/restraints/parameters	6400/0/493	8433/0/591
Goodness of fit on F^2	1.037	1.065
Final R indices [$I > 2\sigma(I)$]	R1 = 0.0360	R1 = 0.0487
R indices (all data)	wR2 = 0.0842	wR2 = 0.1322
Largest diff. peak and hole (e·Å^{-3})	0.379 and –0.308	1.297 and –1.072

Computational Details. Structures of complexes **1–4** were optimized by DFT calculations using the Gaussian 03 program package.[1] The B3LYP density functional method and the 6-31G(d), 6-311G(d,p), or 6-311+G(d,p) basis sets were used for the calculations. The initial models were obtained from the crystal structures. The structures were optimized at the B3LYP/6-31G(d) level. The resulting structures were further optimized at the B3LYP/6-311G(d,p) level, and then at the B3LYP/6-311+G(d,p) level. Optimized structures and selected molecular orbitals of **1–4** for the B3LYP/6-311+G(d,p) calculations are shown in Figures S18–S25, and their molecular coordinates are listed in Tables S3–S6. Harmonic vibrational frequencies were calculated for the optimized geometries using the same level of theory. Time-dependent DFT calculations were performed using the optimized structures at the B3LYP/6-311+G(d,p) level. Calculated electronic transitions for **1–4** are given in Tables S7–S10.

Reference

(1) Gaussian 03, Revision E.01, Frisch, M. J.; Trucks, G. W.; Schlegel, H. B.; Scuseria, G. E.; Robb, M. A.; Cheeseman, J. R.; Montgomery, Jr., J. A.; Vreven, T.; Kudin, K. N.; Burant, J. C.; Millam, J. M.; Iyengar, S. S.; Tomasi, J.; Barone, V.; Mennucci, B.; Cossi, M.; Scalmani, G.; Rega, N.; Petersson, G. A.; Nakatsuji, H.; Hada, M.; Ehara, M.; Toyota, K.; Fukuda, R.; Hasegawa, J.; Ishida, M.; Nakajima, T.; Honda, Y.; Kitao, O.; Nakai, H.; Klene, M.; Li, X.; Knox, J. E.; Hratchian, H. P.; Cross, J. B.; Bakken, V.; Adamo, C.; Jaramillo, J.; Gomperts, R.; Stratmann, R. E.; Yazyev, O.; Austin, A. J.; Cammi, R.; Pomelli, C.; Ochterski, J. W.; Ayala, P. Y.; Morokuma, K.; Voth, G. A.; Salvador, P.; Dannenberg, J. J.; Zakrzewski, V. G.; Dapprich, S.; Daniels, A. D.; Strain, M. C.; Farkas, O.; Malick, D. K.; Rabuck, A. D.; Raghavachari, K.; Foresman, J. B.; Ortiz, J. V.; Cui, Q.; Baboul, A. G.; Clifford, S.; Cioslowski, J.; Stefanov, B. B.; Liu, G.; Liashenko, A.; Piskorz, P.; Komaromi, I.; Martin, R. L.; Fox, D. J.; Keith, T.; Al-Laham, M. A.; Peng, C. Y.; Nanayakkara, A.; Challacombe, M.; Gill, P. M. W.; Johnson, B.; Chen, W.; Wong, M. W.; Gonzalez, C.; Pople, J. A.; Gaussian, Inc., Wallingford CT, 2004.

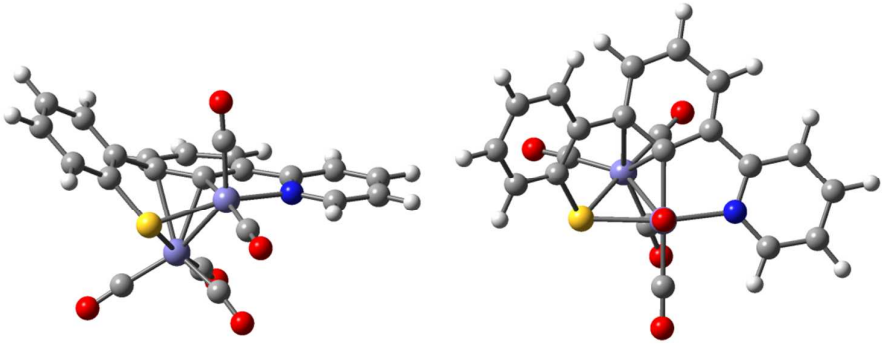

Figure S18. Molecular structures of **1** optimized by the DFT calculation at the B3LYP/6-311+G(d,p) level.

LUMO+2 (–1.788 eV)	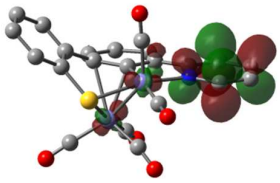	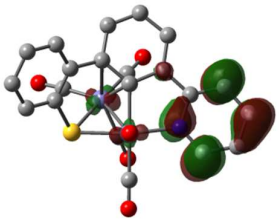
LUMO+1 (–1.986 eV)	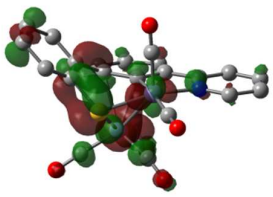	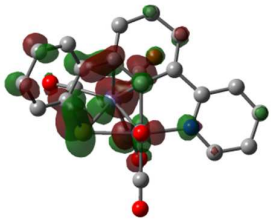
LUMO (–2.585 eV)	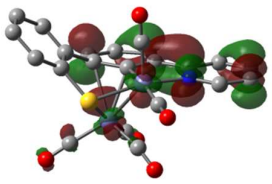	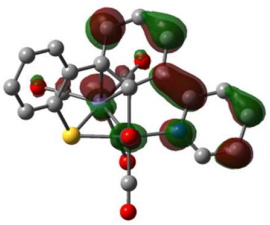

HOMO (–5.640 eV)	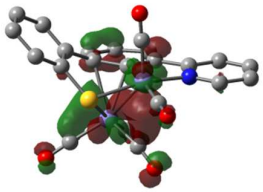	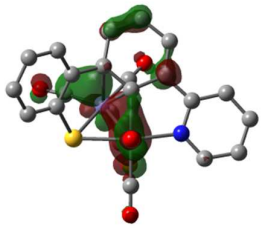
HOMO–1 (–6.144 eV)	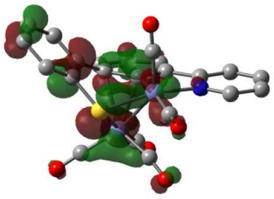	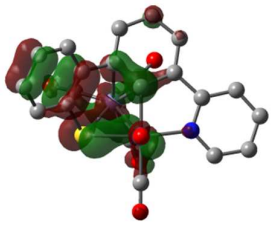
HOMO–2 (–6.602 eV)	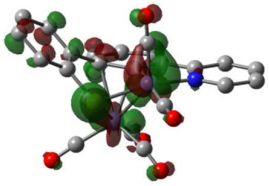	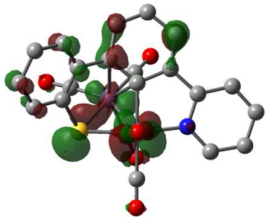
HOMO–3 (–6.661 eV)	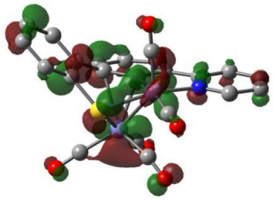	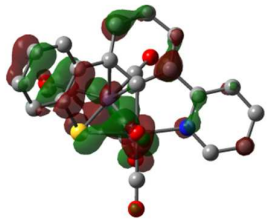
HOMO–4 (–6.918 eV)	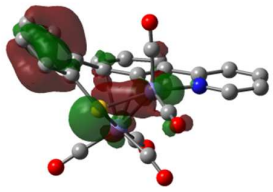	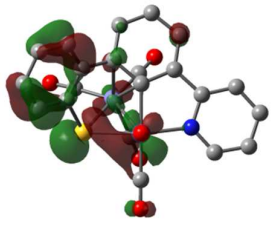

Figure S19. Selected molecular orbitals (isovalue = 0.04) of **1** calculated by DFT at the B3LYP/6-311+G(d,p) level.

Table S3. Molecular coordinates of **1** optimized by the DFT calculation at the B3LYP/6-311+G(d,p) level

	Atomic number	*x*/Å	*y*/Å	*z*/Å
1	8	-1.561402	-0.302907	3.225909
2	8	2.575715	1.712741	3.079791
3	6	1.742285	1.372705	2.371403
4	6	-0.828620	0.013468	2.391725
5	8	-1.517138	-3.520185	1.624338
6	8	-1.027018	3.341037	1.531058
7	6	-0.482872	2.338632	1.440133
8	26	0.393884	0.774869	1.344020
9	16	1.436363	-1.280317	1.045206
10	6	-1.184568	-2.606425	1.021404
11	26	-0.610031	-1.193717	0.007307
12	6	2.662493	-0.883736	-0.189219
13	6	3.791007	-1.692710	-0.306874
14	6	-3.598464	-1.238537	-0.370189
15	7	-2.446021	-0.566945	-0.550407
16	6	-4.825957	-0.762855	-0.799098
17	6	-0.065175	0.512863	-0.805774
18	6	1.243480	1.081492	-0.944399
19	6	2.479177	0.239042	-1.008354
20	6	4.770048	-1.393122	-1.252480
21	6	-2.478298	0.637043	-1.184509
22	6	1.358300	2.432902	-1.393759
23	6	-1.172004	1.282932	-1.310736
24	6	-4.871185	0.469400	-1.450867
25	6	-0.253400	-2.119800	-1.461506
26	6	-3.691682	1.168994	-1.640950
27	6	0.267059	3.151201	-1.826914
28	6	3.465211	0.506479	-1.969085
29	6	-1.004628	2.556190	-1.829778
30	6	4.602101	-0.291792	-2.085745
31	8	0.012019	-2.688913	-2.419451
32	1	-3.527463	-2.191213	0.136842
33	1	-5.719121	-1.348421	-0.624263
34	1	-5.812053	0.874707	-1.804237
35	1	-3.701602	2.125519	-2.145340
36	1	-1.849281	3.124100	-2.202184

37	1	0.387933	4.171271	-2.171998
38	1	2.340214	2.891427	-1.419148
39	1	3.333174	1.334973	-2.654081
40	1	5.347608	-0.055390	-2.836319
41	1	5.651994	-2.017688	-1.335653
42	1	3.905521	-2.545948	0.351709

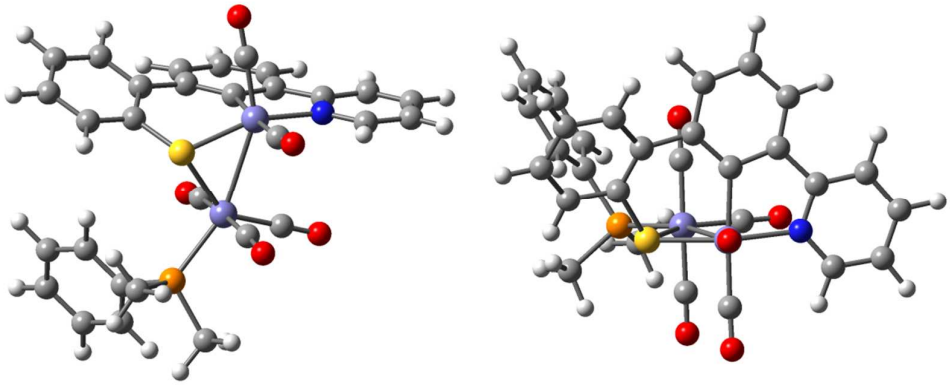

Figure S20. Molecular structures of **2** optimized by the DFT calculation at the B3LYP/6-311+G(d,p) level.

LUMO+2 (–1.438 eV)	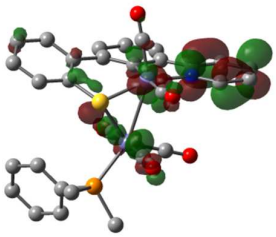	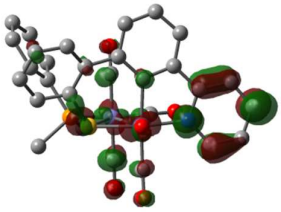
LUMO+1 (–1.466 eV)	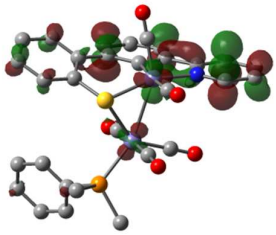	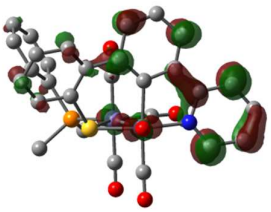
LUMO (–2.008 eV)	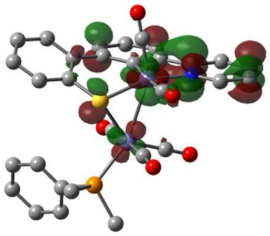	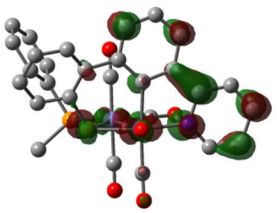

HOMO (–5.135 eV)	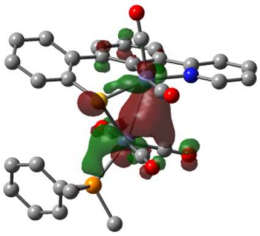	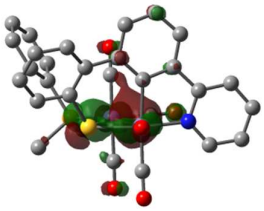
HOMO–1 (–5.759 eV)	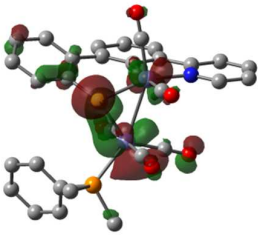	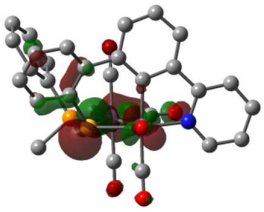
HOMO–2 (–6.009 eV)	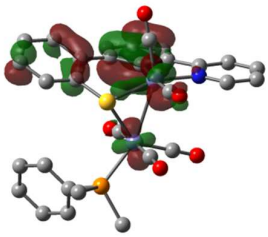	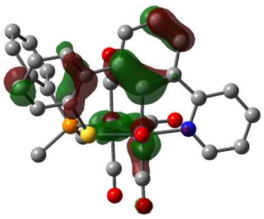
HOMO–3 (–6.153 eV)	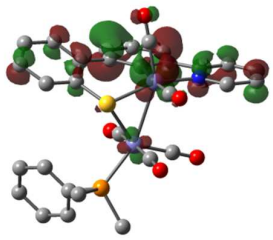	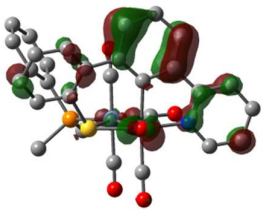
HOMO–4 (–6.328 eV)	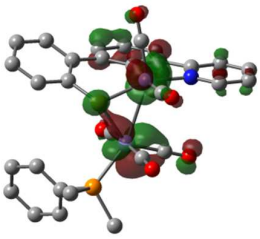	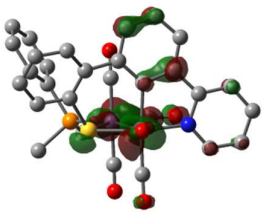

Figure S21. Selected molecular orbitals (isovalue = 0.04) of **2** calculated by DFT at the B3LYP/6-311+G(d,p) level.

Table S4. Molecular coordinates of **2** optimized by the DFT calculation at the B3LYP/6-311+G(d,p) level

	Atomic number	*x*/Å	*y*/Å	*z*/Å
1	6	-1.463433	2.815568	3.043516
2	6	-2.393529	1.796499	2.906389
3	6	-4.375645	-0.420207	2.440241
4	6	5.619429	-0.719274	2.303407
5	6	-5.231370	-1.465717	2.144027
6	6	-0.635232	3.130362	1.974261
7	6	5.816014	0.608823	1.936315
8	6	4.675915	-1.500824	1.636011
9	6	-2.459481	1.081331	1.704835
10	6	-3.415546	-0.006156	1.504284
11	6	0.879004	-0.213844	1.250097
12	6	-0.498828	-2.280434	0.968097
13	6	-5.122538	-2.094181	0.903372
14	6	-0.704252	2.447813	0.743487
15	6	5.057858	1.157888	0.902600
16	6	-1.597230	1.357877	0.610685
17	6	3.915516	-0.961136	0.592613
18	6	2.926209	-3.674372	0.221580
19	6	-4.160823	-1.640279	0.018586
20	6	4.110829	0.382338	0.241144
21	6	0.627888	4.256774	-0.348988
22	6	0.216006	2.907234	-0.334197
23	6	1.551072	4.750981	-1.258994
24	6	0.103275	-2.499834	-1.453378
25	6	0.735199	2.078653	-1.352217
26	6	-2.770823	1.446906	-1.628874
27	6	3.340839	-1.953091	-2.027324
28	6	2.101753	3.900876	-2.216441
29	6	1.676076	2.580908	-2.265066
30	6	-2.281018	-1.020608	-2.307524
31	1	-1.373805	3.356912	3.978157
32	1	-3.046008	1.556834	3.737966
33	1	-4.443717	0.082214	3.395035
34	1	6.198380	-1.152826	3.111197
35	1	-5.972347	-1.789082	2.865926
36	1	6.548995	1.215346	2.455972

37	1	4.542193	-2.531083	1.941304
38	1	0.109314	3.903622	2.115936
39	1	2.622555	-3.803933	1.261249
40	1	-5.765612	-2.917962	0.622048
41	1	0.187345	4.943889	0.361701
42	1	5.194653	2.194517	0.616511
43	1	3.970253	-3.972996	0.101381
44	1	2.298716	-4.322831	-0.392649
45	1	-4.051928	-2.104916	-0.951678
46	1	3.512301	0.836308	-0.541191
47	1	1.826290	5.799300	-1.230454
48	1	4.378669	-2.292709	-2.016894
49	1	3.293107	-0.949188	-2.449483
50	1	2.745122	-2.616205	-2.657381
51	1	2.822272	4.268261	-2.938382
52	1	2.044998	1.921832	-3.043023
53	7	-3.321673	-0.624120	0.296456
54	8	1.221866	0.358608	2.178598
55	8	-1.110590	-2.920112	1.708256
56	8	-0.060382	-3.327967	-2.233935
57	8	-3.318630	2.347073	-2.082469
58	8	-2.616855	-1.637236	-3.213509
59	15	2.637584	-1.933389	-0.316005
60	16	0.173177	0.421396	-1.730304
61	26	0.456608	-1.296852	-0.155898
62	26	-1.883788	0.102001	-0.919652

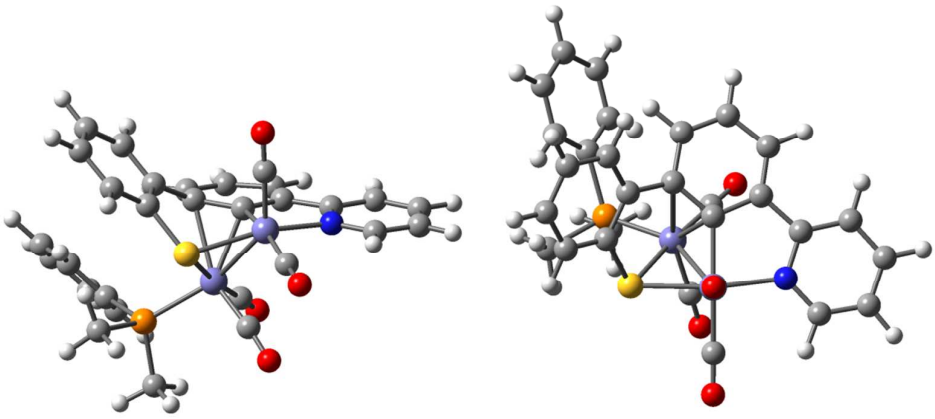

Figure S22. Molecular structures of **3** optimized by the DFT calculation at the B3LYP/6-311+G(d,p) level.

LUMO+2 (–1.434 eV)	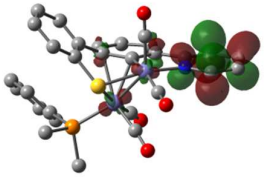	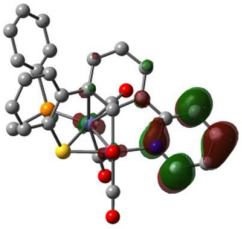
LUMO+1 (–1.561 eV)	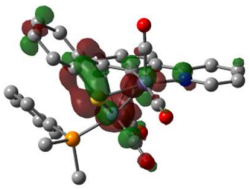	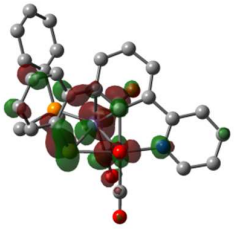
LUMO (–2.154 eV)	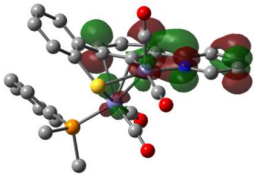	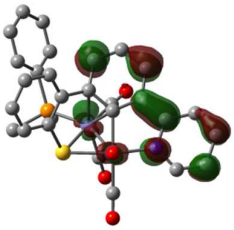

HOMO (–4.979 eV)	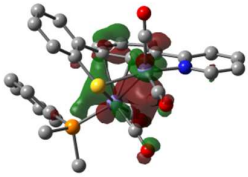	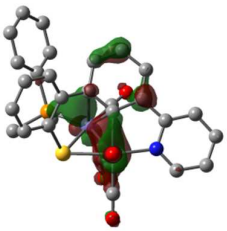
HOMO–1 (–5.716 eV)	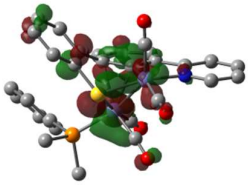	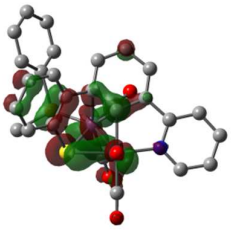
HOMO–2 (–6.137 eV)	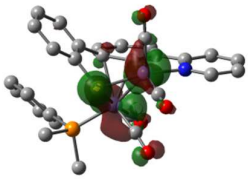	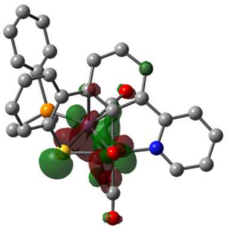
HOMO–3 (–6.217 eV)	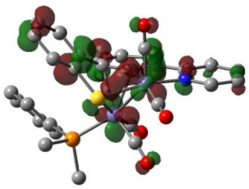	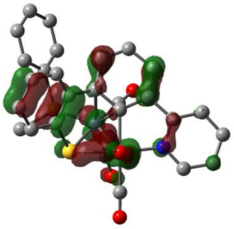
HOMO–4 (–6.394 eV)	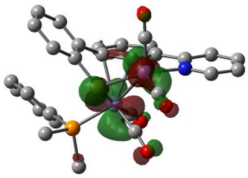	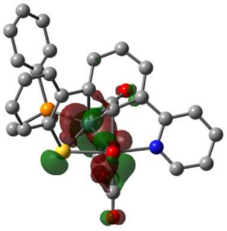

Figure S23. Selected molecular orbitals (isovalue = 0.04) of **3** calculated by DFT at the B3LYP/6-311+G(d,p) level.

Table S5. Molecular coordinates of **3** optimized by the DFT calculation at the B3LYP/6-311+G(d,p) level

	Atomic number	*x*/Å	*y*/Å	*z*/Å
1	6	5.077153	-2.359607	-1.578039
2	6	-2.438614	-2.030812	2.873336
3	6	3.774617	-2.208264	-2.019627
4	6	-0.122417	-2.249295	0.396898
5	6	-4.921364	-2.504840	-0.884521
6	6	-3.922731	-2.274961	0.059630
7	6	0.857266	-1.771169	-2.714258
8	6	-0.514248	-1.549539	-2.934485
9	6	5.527722	-1.563143	-0.523641
10	6	2.930742	-1.266758	-1.412319
11	6	1.536978	-1.023817	-1.770171
12	6	0.875006	-0.916906	2.255560
13	6	-5.604064	-1.434566	-1.459383
14	6	-3.592053	-0.969603	0.449841
15	6	-1.152773	-0.523137	-2.279265
16	6	4.650618	-0.651002	0.036520
17	6	0.896331	0.029843	-1.016092
18	6	-0.467204	0.339295	-1.365477
19	6	-5.276415	-0.132092	-1.087278
20	6	-4.277048	0.099446	-0.144091
21	6	-2.845568	0.770088	2.630148
22	6	2.995978	1.233299	1.849890
23	6	-1.033759	1.712452	-1.186333
24	6	2.586034	2.200231	-0.654993
25	6	-1.774604	2.317178	-2.213100
26	6	-0.773166	2.478269	-0.040287
27	6	-2.265923	3.616266	-2.089129
28	6	-1.245844	3.784434	0.083054
29	6	-2.004352	4.354767	-0.938704
30	1	5.734448	-3.083720	-2.045218
31	1	-2.148316	-2.989024	2.441653
32	1	3.402220	-2.811543	-2.836369
33	1	-5.165411	-3.522457	-1.168772
34	1	-3.403727	-3.124492	0.487395
35	1	1.355004	-2.561290	-3.265195
36	1	-3.472039	-2.089017	3.221891

37	1	-1.778973	-1.834833	3.721170
38	1	-1.060556	-2.179968	-3.626186
39	1	6.536819	-1.642527	-0.140421
40	1	-6.383570	-1.613989	-2.191205
41	1	-2.201934	-0.338695	-2.480325
42	1	4.967375	-0.015443	0.852409
43	1	-3.851232	0.569121	3.006058
44	1	-2.164853	0.933367	3.467167
45	1	-5.798052	0.708910	-1.530502
46	1	-4.033039	1.121787	0.117763
47	1	-2.853981	1.677837	2.028031
48	1	-1.948398	1.775951	-3.135100
49	1	-2.836432	4.053225	-2.901064
50	1	-1.023755	4.347545	0.982643
51	1	-2.376564	5.367956	-0.837183
52	7	3.380552	-0.496547	-0.383460
53	8	-0.153250	-3.371938	0.147019
54	8	1.408565	-1.275250	3.217230
55	8	3.595297	1.523609	2.783684
56	8	2.891235	3.088402	-1.314875
57	15	-2.220154	-0.662465	1.648627
58	16	0.167673	1.745455	1.287495
59	26	-0.100513	-0.529266	0.837984
60	26	2.049286	0.836262	0.338157

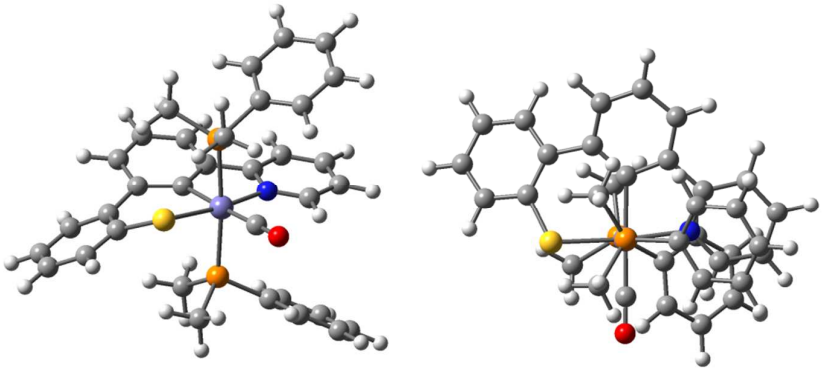

Figure S24. Molecular structures of **4** optimized by the DFT calculation at the B3LYP/6-311+G(d,p) level.

LUMO+2 (–1.063 eV)	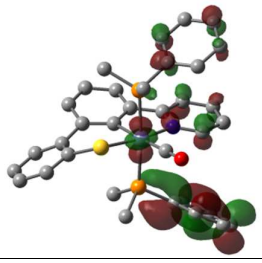	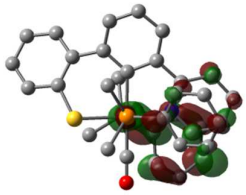
LUMO+1 (–1.358 eV)	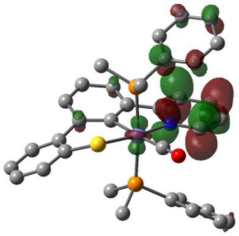	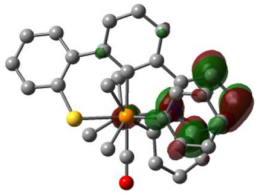
LUMO (–1.640 eV)	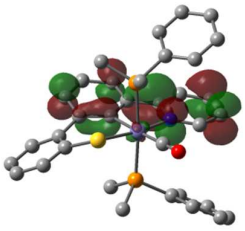	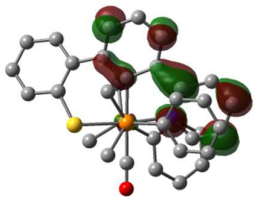

HOMO (–4.570 eV)	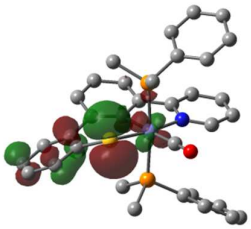	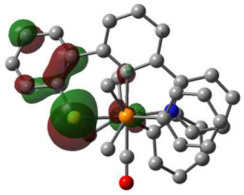
HOMO–1 (–5.582 eV)	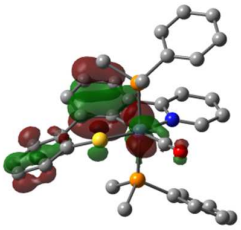	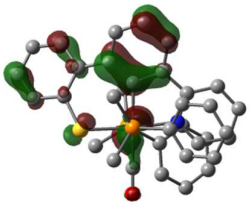
HOMO–2 (–5.829 eV)	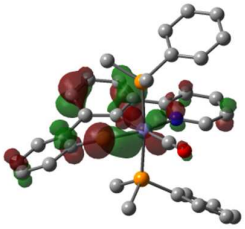	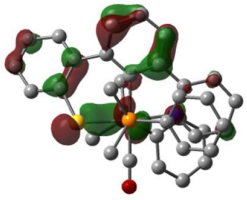
HOMO–3 (–5.921 eV)	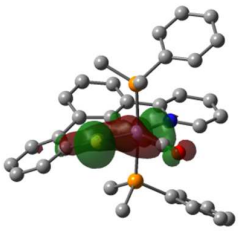	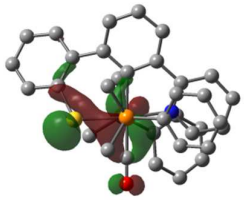
HOMO–4 (–6.140 eV)	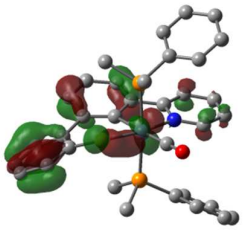	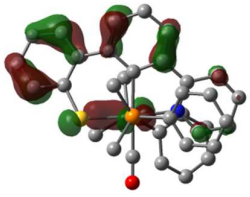

Figure S25. Selected molecular orbitals (isovalue = 0.04) of **4** calculated by DFT at the B3LYP/6-311+G(d,p) level.

Table S6. Molecular coordinates of **4** optimized by the DFT calculation at the B3LYP/6-311+G(d,p) level

	Atomic number	*x*/Å	*y*/Å	*z*/Å
1	6	-5.677610	-1.427491	0.863057
2	6	-4.414371	-1.492449	1.433785
3	6	-2.330483	1.982115	1.435465
4	6	-0.837696	-2.391677	3.432344
5	6	-1.923733	-2.331260	2.562449
6	6	0.274935	-1.604346	3.182319
7	6	-5.790214	-1.231425	-0.513705
8	6	0.918821	5.078449	1.431701
9	6	0.096215	3.958782	1.314321
10	6	-3.223584	-1.381692	0.682773
11	6	-1.927634	-1.515615	1.413186
12	6	0.317906	-0.839538	2.006324
13	6	2.530540	0.295148	2.550769
14	6	1.365685	5.743821	0.292823
15	6	-0.296363	3.483724	0.056471
16	6	-0.736482	-0.831956	1.053155
17	6	-4.641717	-1.066122	-1.271908
18	6	1.460905	0.018586	1.685896
19	6	3.545847	1.147550	2.151456
20	6	-3.351863	-1.117590	-0.703399
21	6	-2.608117	2.529229	-1.347063
22	6	0.986230	5.279365	-0.965729
23	6	0.167061	4.158618	-1.082670
24	6	3.480775	1.726001	0.884873
25	6	2.398886	1.418377	0.077136
26	6	2.986681	-3.105476	0.268500
27	6	0.004131	-3.546963	-0.610193
28	6	4.334854	-3.265278	0.588788
29	6	0.368166	0.765466	-2.211997
30	6	2.594132	-2.269305	-0.784132
31	6	5.314108	-2.589804	-0.134783
32	6	3.590407	-1.582108	-1.493594
33	6	4.936343	-1.744537	-1.177301
34	6	0.859452	-2.375631	-3.054401
35	26	-0.179721	0.033074	-0.671465
36	7	1.409089	0.589370	0.452027

37	15	-1.345734	1.965856	-0.123885
38	15	0.814459	-2.018746	-1.239711
39	16	-2.017337	-0.849071	-1.833038
40	1	-6.560458	-1.515179	1.486142
41	1	-4.343396	-1.611838	2.508005
42	1	-2.748303	2.974577	1.618886
43	1	-0.873104	-3.038216	4.302049
44	1	-1.715844	1.672983	2.280638
45	1	-2.787396	-2.948827	2.778264
46	1	-3.139908	1.258950	1.331535
47	1	1.207154	5.430298	2.416192
48	1	-0.239326	3.460959	2.215798
49	1	1.105001	-1.612612	3.880169
50	1	-6.764315	-1.182248	-0.988617
51	1	2.554674	-0.156662	3.532977
52	1	-3.030133	3.489387	-1.042139
53	1	2.001625	6.617211	0.383977
54	1	4.374010	1.362640	2.817177
55	1	-4.719924	-0.883483	-2.337975
56	1	-3.392653	1.775275	-1.405651
57	1	-2.163741	2.620234	-2.338211
58	1	1.325612	5.790566	-1.859962
59	1	-0.110214	3.815661	-2.072680
60	1	4.244156	2.404330	0.526620
61	1	-0.032155	-3.551867	0.478262
62	1	2.244408	-3.643170	0.845202
63	1	4.617047	-3.923543	1.403293
64	1	-1.019934	-3.544846	-0.984148
65	1	2.309474	1.854431	-0.908465
66	1	6.362264	-2.719720	0.110309
67	1	0.529690	-4.433183	-0.972796
68	1	3.319818	-0.917083	-2.306498
69	1	5.690181	-1.211647	-1.746483
70	1	-0.166020	-2.360963	-3.425697
71	1	1.431897	-1.615037	-3.585534
72	1	1.306206	-3.354643	-3.238785
73	8	0.700747	1.230051	-3.215712

Table S7. Energies of electronic transitions of **1** calculated by TD-DFT at the B3LYP/6-311+G(d,p) level

State	Component (coefficient) [a]	*E*/eV	λ/nm	f [b]
1 (singlet-A)	H–6→L (-0.10859) H–6→L+3 (-0.11006) H–2→L (-0.23024) H–2→L+1 (0.22959) H–2→L+3 (-0.21408) H–1→L (-0.20336) H–1→L+1 (0.14475) H–1→L+3 (-0.14521) H→L (0.14438) H→L+1 (0.26830)	2.2100	561.01	0.0008
2 (singlet-A)	H–2→L (0.11325) H–2→L+1 (-0.12754) H–2→L+3 (0.10239) H–1→L (0.10854) H→L (0.48611) H→L+1 (0.26164) H→L+3 (0.12231)	2.2285	556.37	0.0453
3 (singlet-A)	H–2→L (0.15946) H–1→L (-0.35547) H→L+1 (0.48328) H→L+2 (0.12610)	2.4052	515.48	0.0320
4 (singlet-A)	H–7→L+1 (-0.18250) H–1→L (0.43860) H–1→L+1 (0.31469) H–1→L+3 (0.10869)	2.5970	477.41	0.0081
5 (singlet-A)	H–6→L (-0.20708) H–6→L+1 (0.22451) H–6→L+3 (-0.17925) H–6→L+4 (0.10873) H–6→L+5 (-0.12384) H–6→L+6 (-0.10685) H–5→L+1 (-0.15709) H–5→L+3 (0.10377) H–4→L+1 (-0.14086) H–3→L (0.13039) H–3→L+1 (-0.15557) H–3→L+3 (0.11570) H–1→L (0.15356)	2.6636	465.47	0.0012

[a] H = HOMO, L = LUMO. [b] Oscillator strength.

Table S8. Energies of electronic transitions of **2** calculated by TD-DFT at the B3LYP/6-311+G(d,p) level

State	Component (coefficient) [a]	E/eV	λ/nm	f [b]
1 (singlet-A)	H–5→L (-0.11238) H–4→L (-0.22859) H–4→L+1 (-0.12771) H–4→L+2 (-0.13482) H–3→L (0.23955) H–3→L+1 (0.12650) H–3→L+2 (0.12701) H–2→L (-0.10107) H–1→L (0.20430) H–1→L+1 (0.10517) H–1→L+2 (0.11992) H–1→L+4 (-0.13272) H→L (-0.21247) H→L+2 (-0.11936)	2.2073	561.70	0.0281
2 (singlet-A)	H–1→L (0.29699) H–1→L+1 (0.12837) H–1→L+2 (0.13686) H→L (0.44267) H→L+2 (0.18015) H→L+3 (-0.11030) H→L+4 (0.14405)	2.3250	533.27	0.0593
3 (singlet-A)	H–5→L (0.24628) H–5→L+1 (0.12316) H–5→L+2 (0.11631) H–5→L+4 (-0.14978) H–2→L (-0.10420) H–1→L (0.15438) H→L+1 (0.17118) H→L+2 (-0.20284) H→L+3 (0.22590) H→L+4 (-0.22230) H→L+5 (-0.14290)	2.5957	477.66	0.0127
4 (singlet-A)	H–6→L (0.10689) H–3→L (-0.15269) H–2→L (0.36080) H–2→L+1 (0.16252) H–2→L+2 (0.12996) H–1→L (0.29712) H–1→L+2 (0.10715) H→L (-0.24954) H→L+1 (0.10927)	2.6717	464.06	0.0246

5 (singlet-A)	H–6→L (0.11361) H–5→L (0.25247) H–5→L+1 (0.15313) H–5→L+2 (0.12940) H–5→L+4 (-0.14581) H–4→L (-0.10663) H→L (-0.23064) H→L+2 (0.28454) H→L+3 (-0.22264)	2.7194	455.92	0.0414
6 (singlet-A)	H–6→L (-0.17475) H–6→L+1 (-0.10651) H–4→L (0.30440) H–4→L+1 (0.12363) H–4→L+2 (0.13337) H–2→L (-0.20795) H–1→L (0.17770) H→L (-0.23634) H→L+1 (0.15484) H→L+2 (0.23907)	2.7862	444.99	0.0179
7 (singlet-A)	H–4→L (-0.13648) H–1→L (-0.20247) H→L+1 (0.46974) H→L+2 (0.24958) H→L+3 (0.10931) H→L+4 (0.12790) H→L+9 (-0.13278)	2.9311	423.00	0.0382

[a] H = HOMO, L = LUMO. [b] Oscillator strength.

Table S9. Energies of electronic transitions of **3** calculated by TD-DFT at the B3LYP/6-311+G(d,p) level

State	Component (coefficient) [a]	*E*/eV	λ/nm	f [b]
1 (singlet-A)	H→L (0.58589) H→L+1 (-0.18252) H→L+3 (0.12834)	2.0592	602.10	0.0755
2 (singlet-A)	H–2→L (0.16062) H–2→L+1 (0.19306) H–1→L (0.14010) H–1→L+1 (0.12421) H→L (0.16096) H→L+1 (0.47108)	2.1332	581.21	0.0236
3 (singlet-A)	H–3→L+1 (-0.11768) H–2→L (-0.12387) H–2→L+1 (-0.19040) H–2→L+4 (-0.10163) H–1→L (-0.23625) H–1→L+1 (-0.24627) H→L (0.11212) H→L+1 (0.35373)	2.2110	560.77	0.0053
4 (singlet-A)	H–7→L+1 (-0.13979) H–6→L+1 (0.11177) H–1→L (0.39523) H–1→L+1 (-0.34058) H–1→L+3 (0.13869)	2.5662	483.14	0.0025
5 (singlet-A)	H–6→L (-0.11122) H–6→L+1 (-0.11025) H–5→L (0.11035) H–5→L+1 (0.18393) H–4→L+1 (0.21500) H–3→L (-0.18479) H–3→L+1 (-0.11672) H–2→L (0.18235) H–1→L+1 (-0.14851) H→L (-0.11481) H→L+2 (0.13979) H→L+3 (0.16937)	2.6379	470.01	0.0035

[a] H = HOMO, L = LUMO. [b] Oscillator strength.

Table S10. Energies of electronic transitions of **4** calculated by TD-DFT at the B3LYP/6-311+G(d,p) level

State	Component (coefficient) [a]	*E*/eV	λ/nm	f [b]
1 (singlet-A)	H–4→L+2 (-0.11999) H–4→L+8 (-0.10713) H–2→L+2 (0.15291) H–2→L+8 (0.13226) H→L+1 (-0.19942) H→L+2 (0.28556) H→L+6 (0.14323) H→L+7 (0.10359) H→L+8 (0.19899)	1.9619	631.96	0.0008
2 (singlet-A)	H→L (0.69250)	2.3102	536.69	0.0012
3 (singlet-A)	H→L+1 (0.64565) H→L+2 (0.13259)	2.6644	465.34	0.0082
4 (singlet-A)	H–5→L+2 (-0.10002) H–5→L+8 (-0.14025) H–3→L+1 (-0.13120) H–3→L+2 (0.23301) H–3→L+6 (0.15998) H–3→L+7 (0.14395) H–3→L+8 (0.23652) H–3→L+9 (-0.10822) H–3→L+10 (0.14861) H–3→L+21 (-0.10896) H→L+1 (-0.10378) H→L+2 (-0.13442) H→L+3 (0.10383)	2.8344	437.43	0.0022
5 (singlet-A)	H–6→L+2 (0.14519) H–1→L+1 (-0.16423) H–1→L+2 (0.25420) H–1→L+8 (0.13713) H→L+2 (0.39050)	2.9129	425.64	0.0137
6 (singlet-A)	H–6→L+2 (-0.12322) H–1→L+1 (0.16412) H–1→L+2 (-0.21200) H→L+2 (0.36295) H→L+5 (0.11528) H→L+6 (-0.14855) H→L+8 (-0.15263)	3.0205	410.48	0.0018
7 (singlet-A)	H→L+3 (0.56791) H→L+5 (-0.24864)	3.1858	389.17	0.0052

	H→L+6 (0.18774)			
8 (singlet-A)	H–2→L (0.14101) H–1→L (0.60782) H–1→L+1 (0.10573)	3.2531	381.13	0.0412
9 (singlet-A)	H–3→L (-0.10583) H–1→L (-0.13941) H→L+2 (-0.16394) H→L+4 (0.48212) H→L+6 (0.12472) H→L+7 (-0.11929) H→L+9 (0.12366) H→L+10 (-0.19225)	3.3089	374.70	0.0083
10 (singlet-A)	H→L+3 (0.24486) H→L+4 (0.21788) H→L+5 (0.44315) H→L+6 (-0.19370) H→L+7 (0.23882) H→L+10 (0.11674)	3.3397	371.25	0.0070

[a] H = HOMO, L = LUMO. [b] Oscillator strength.

Table S11. Charge Distributions Calculated by Natural Population Analysis for **1**, **2**, and **3**[a]

Basis set	6-311G(d,p)			6-311+G(d,p)		
Complex	**1**	**2**	**3**	**1**	**2**	**3**
Fe1[b]	0.639	0.643	0.643	-0.090	-0.048	-0.073
Fe2[b]	0.474	0.330	0.488	-0.287	-0.532	-0.335
PyBPT[c]	-0.707	-0.671	-0.881	-0.281	-0.339	-0.432
$(CO)_n$[c]	-0.406	-0.530	-0.467	0.658	0.522	0.453
PMe_2Ph[c]		0.228	0.217		0.397	0.387
Δ(Fe1-Fe2)[d]	0.165	0.313	0.155	0.197	0.484	0.262

[a] Structures optimized at the B3LYP/6-311+G(d,p) level were used. [b] Fe1 is in the $Fe(PyBPT)(CO)_2$ unit, and Fe2 is in the $Fe(CO)_n(PMe_2Ph)_m$ unit (**1**, $n = 3$, $m = 0$; **2**, $n = 3$, $m = 1$; **3**, $n = 2$, $m = 1$). [c] Sum of the atomic charges on the ligand. [d] Differences in atomic charge between Fe1 and Fe2.

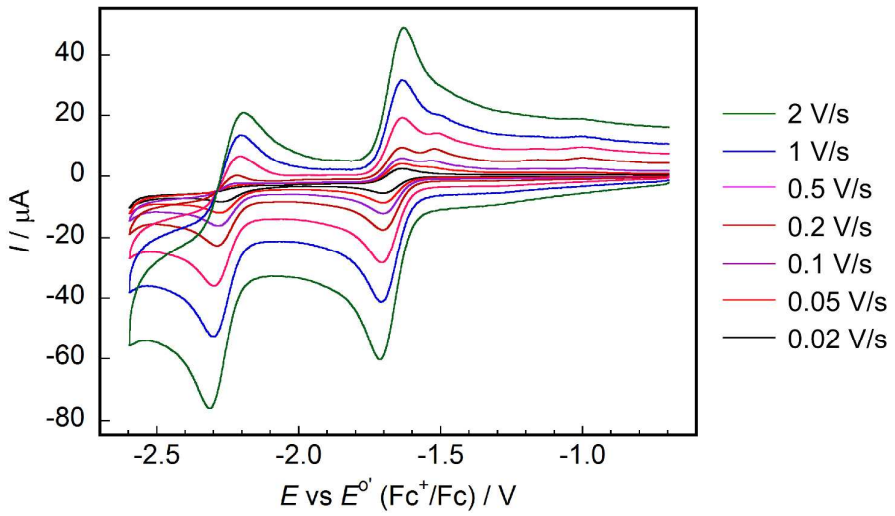

Figure S26. The reduction processes of **3** recorded at scan rates from 0.02 to 2 V s^{-1}.

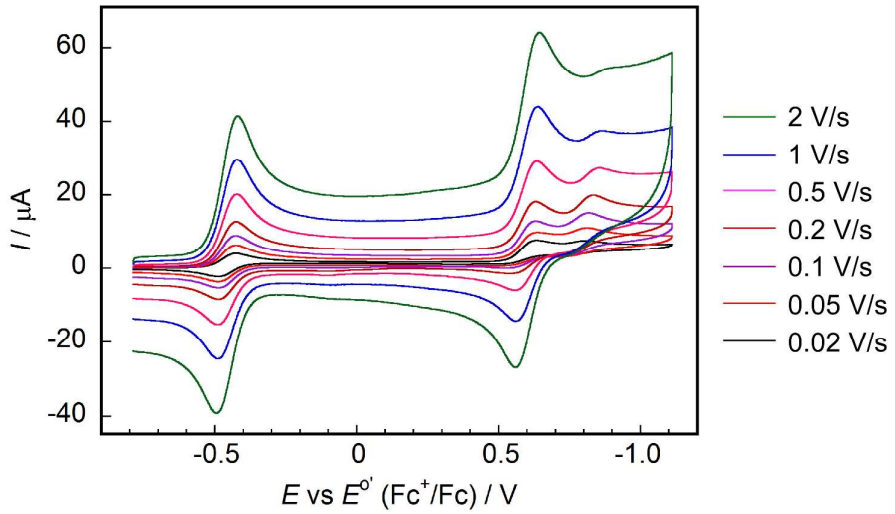

Figure S27. The oxidation processes of **4** recorded at scan rates from 0.02 to 2 V s^{-1}.